J. Micropalaeontology, 43, 55–68, 2024
https://doi.org/10.5194/jm-43-55-2024

Journal of Micropalaeontology
Open Access

Nannofossils from the Middle Eocene Sabiñánigo Sandstone Formation in the Jaca Basin (southern Pyrenees): biostratigraphy and paleoenvironmental implications

Elizabeth R. Lasluisa[1], Oriol Oms[2], Eduard Remacha[2], Alba González-Lanchas[3], Hug Blanchar-Roca[2], and José Abel Flores[1]

[1]Departamento de Geología, Facultad de Ciencias, Universidad de Salamanca, Salamanca, 37008, Spain
[2]Departament de Geología, Universitat Autònoma de Barcelona, Bellaterra (Barcelona), 08193, Spain
[3]Department of Earth Sciences, University of Oxford, Oxford, United Kingdom

Correspondence: Elizabeth R. Lasluisa (lasluisae@usal.es)

Received: 8 July 2023 – Revised: 30 January 2024 – Accepted: 15 February 2024 – Published: 11 April 2024

Abstract. This study presents the first detailed data on calcareous nannofossil assemblages from the Sabiñánigo Sandstone Formation in the Jaca Basin (central south Pyrenees). This formation is mainly composed of deltaic and outer-shelf sediments. These siliciclastic deposits contain nannofossil assemblages that are moderately to well-preserved, particularly in fine-grained levels. They contain a calcareous nannofossil assemblage dominated by the species *Cyclicargolithus floridanus*, *Coccolithus pelagicus*, *Coccolithus formosus*, *Clausicoccus fenestratus*, *Zygrhablithus bijugatus*, and several species of *Sphenolithus* and *Chiasmolithus*. The biostratigraphic results enabled the characterization of the Middle Eocene biohorizons, based on global stratigraphic scales and the improvement of the temporal correlation and lateral evolution of this basin's deposits. The sedimentary sequence of the Sabiñánigo Sandstone was deposited during the Middle Eocene, between the upper part of biozone NP16 and the base of NP17, in the Bartonian. The calcareous nannoplankton assemblage suggests warm and oligotrophic surface waters for the Bartonian interval in the Jaca Basin.

1 Introduction

The global Eocene climatic evolution from greenhouse to icehouse conditions (see the compilation in Henehan et al., 2019) contains several events which have a variable impact on the biotic record. These changes are rather well understood for the deep oceanic settings (Bohaty et al., 2009; Boscolo Galazzo et al., 2013, 2014; Moebius et al., 2014; Stokke et al., 2020), but shallow marine environments have been largely overlooked. These latter environments can potentially shed light on bioevents controversies, such as those taking place during the Middle Eocene (ca. 40 Ma).

The Sabiñánigo Sandstone (southern Pyrenees, Spain) is a good location to explore such events in deltaic settings. This sandstone is an excellent guide level, consisting of fine sand and silt deposits intercalated with clays and silts of an outer shelf which outcrops in the northernmost area of the Jaca Basin (Pyrenees, Spain). So far, biostratigraphic data from the Sabiñánigo Sandstone are very limited. Canudo and Molina (1988) studied planktonic foraminifera in this basin and placed the Sabiñánigo Sandstone at the base of the Bartonian (*T. rohri* zone, which defines P13–P14, according to the Blow (1979) scale). Puigdefábregas (1975) associates this formation with the strata of the Capana Formation of the Biarritzian age (between the Lutetian and Bartonian). All magnetostratigraphic studies placed the Sabiñánigo Sandstone in the C18n–C18r polarity reversal (Bartonian), e.g., Oms et al. (2003) at Latas section and Hogan and Burbank (1996) and Vinyoles et al. (2021) at the nearby Yebra de Basa section.

2 Geology settings and stratigraphy

The Jaca Basin, also known as the Jaca–Pamplona Basin, is part of the south Pyrenean foreland basin system that developed west of the Boltaña Anticline (Fig. 1). The structural characteristics of the Jaca Basin have been established by Seguret (1972), Labaume (1983), Labaume et al. (1985), Cámara and Klimowith (1985), Teixell (1996), Teixell and García-Sansegundo (1995), Cámara and Flinch (2017), and Labaume and Teixell (2018). The basin extends along a broad, complex, and asymmetric syncline with an ESE–WNW direction, whose limbs have different structural and stratigraphic characteristics. The axis of the syncline, which contains the Jaca Basin, is determined by the position of the Paleozoic cutoff of the Guarga thrust.

The Eocene marine clastic sedimentation of the northern Guarga syncline is dominated by the deep systems of the Hecho Group, which has been divided into the Lower Hecho Group and Upper Hecho Group by Remacha et al. (2003). The youngest representative of the Upper Hecho Group is the Rapitán system (Remacha et al., 1987, 1991, 2003) (Fig. 3), dated as Bartonian by Oms et al. (2003) and Gonzalez-Lanchas et al. (2019). The Rapitán system transitions vertically and transitionally to the Larrés Marls (Remacha et al., 1987), consisting of very thin turbiditic and shaly layers corresponding to a slope fan. The top of the Larrés Marls evolves progressively to the Sabiñánigo Sandstone.

The Sabiñánigo Sandstone was defined by Hehuwat (1970) and has been studied and/or mapped by Puigdefàbregas (1975), Remacha et al. (1987), Remacha and Picart (1991), Lafont (1994), Gil-Peña et al. (1990), Montes-Santiago (2002), Bauer (2007), and Boya (2018). As growth strata show, the Sabiñánigo Sandstone was confined to the north by a relief resulting from the early Oturia thrust (whose present location is due to a reactivation). Several pulses of this structure are likely to have been the main controllers of the sequential arrangement of the Sabiñánigo Sandstone.

The Sabiñánigo Sandstone Formation at the Latas section

The studied stratigraphic section (Latas section, lat. 42°31.278′ N, long. 0°19.614′ W) is exposed on the road between the localities of Sabiñánigo and Lárrede in the province of Huesca, Spain. This site was introduced by Remacha and Picart (1991), who described a 130 m thick section displaying high-quality outcrops that allow a continuous facies analysis. The main lithologies are fine sands, clays, and silts that are here represented in the stratigraphic section (Figs. 3 and 4).

The lowest 2 m of the studied section consists of calcareous coarse-grained siltstones and fine-grained sandstones intercalated with shaly marls. Occasionally, the sandstone presents hummocky cross-stratification and wave and current ripples, and their marly sections may reach regions close to the platform edge.

Above this are 20 m of cycles that typically begin with marly fine-grained sandstone and siltstone, passing up into coarse-grained sandstone. In the lowest part of this unit, there is a distinctive stratum with ball-and-pillow structure, which also conserves hummocky cross-stratification, planar cross-stratification, and wave and current ripples. These cycles (Remacha and Picart, 1991) are typically interpreted as delta front deposits (delta lobes).

Around 23 m from the bottom of the section, the facies change and begin with a bioclastic and bioturbated sandstone bed, followed by calcareous gray fine-grained sandstones intercalated with fine-grained siltstones, with marly divisions at the base that gradually disappear toward the top. The top of this unit has decametric and metric beds of massive fine-grained siltstones and sandstones. The basal, middle, and upper parts of this unit (marked with an asterisk in Figs. 3 and 4) contain, among other things, layers of benthic foraminifera of the genera *Nummulites* and *Assilina*.

At 82 m from the bottom of the section, the features of the unit are similar to those described above in the first 20 m of the section. Unlike the beds of the lower unit, these deposits maintain their waxing and waning character, and in many cases, there are incomplete sequences at the base due to erosion.

The upper Sabiñánigo Sandstone Formation has a comparatively more monotonous character, with coarse-grained sandstones alternating with shales. These facies also present, to some extent, similar characteristics to those described above in the first 20 m of the section. This unit also has a stratum with ball-and-pillow structure, and the beds preserve hummocky cross-stratification, planar cross-stratification, wave and current ripples, mega ripples, and climbing ripples. In the uppermost part, there is a significant increase in shale. These observations indicate that such delta front deposits record a transition between distributary mouth bars and distributary channel deposits. Refinements by Boya (2018) considered muddier intervals (meters 23 to 82) to record other shelf environments, while the sandier delta front intervals (from the base to meter 23 and meter 82 to the top) also identified hyperpycnal processes and delta lobe deposition.

3 Materials and methods

The Latas section is ca. 130 m thick, and a total of 40 samples were collected from fine-grain rock levels, such as pelagic shales and siltstone, where mixing with reworked materials was minimal. The calcareous nannofossil samples were prepared using the settling method of Flores and Sierro (1997). The samples were analyzed under a LEICA DMRXE polarized microscope at 1000× and 1250× magnification. To estimate the abundance of nannofossils in the samples, around 500 specimens (autochthonous and reworked) were counted

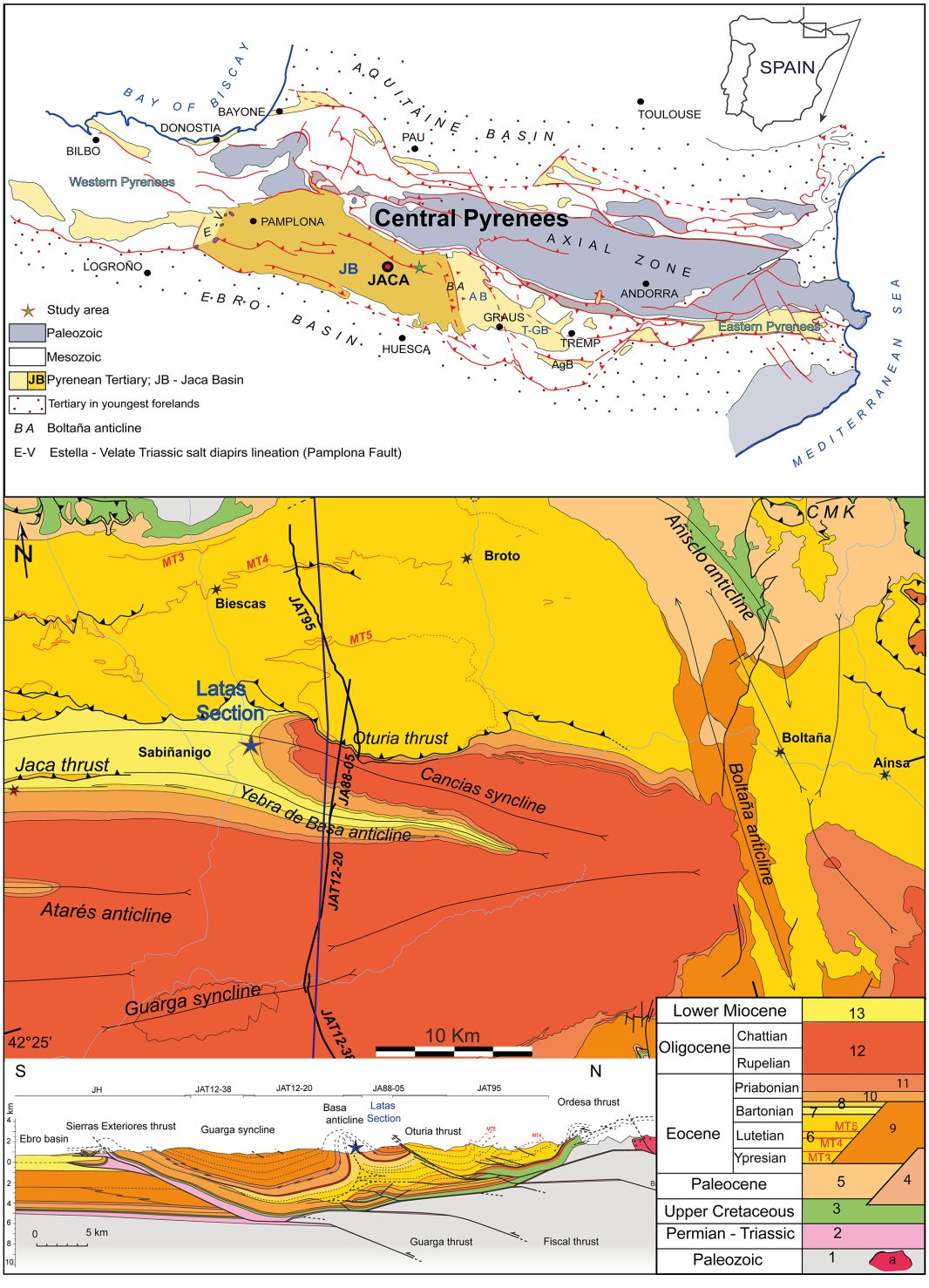

Figure 1. Geological context of the study section. Top: schematic map of the location of the southern Pyrenees and the Jaca Basin. Center: geological map of the Jaca Basin showing the main stratigraphic units; the star marks the location of the Sabiñánigo Sandstone Formation in the study area, as exposed along the road from Sabiñánigo (Sardas Bridge) to Lárrede. Bottom: cross section of the Jaca Basin and the location of the Latas section. Modified from Labaume and Teixell (2018).

and classified in each smear slide. This procedure was carried out due to the high percentage of reworked material and to guarantee the recognition of every taxon exceeding 1 % of the total assemblage (Denisson and Hay, 1967; Flores and Sierro, 1997).

The abundance patterns of biostratigraphically significant taxa are expressed as percentages (%) calculated in relation to the total number of nannofossils in each sample.

The taxonomic criteria followed are mainly based on "Cenozoic calcareous nannofossils" (Perch-Nielsen, 1985), *Calcareous nannofossil biostratigraphy* (Bown, 1998), and the updated online dataset Nannotax (https://www.mikrotax.org/Nannotax3/index.html, last access: 18 January 2024). In this study, calcareous nannofossils include all heterococcoliths, holococcoliths, and nannoliths incertae sedis.

Cretaceous and Paleocene taxa were readily classified as reworked. Also, several nannofossil species belonging to the Early Eocene NP10 to NP14 zones were identified. These included *Toweius* (e.g., *T. pertusus*, *T. gammation*), *Tribrachiatus orthostylus*, *Chiasmolithus bidens*, and some discoasters (e.g., *D. araneus* and *D. multiradiatus*) and are interpreted as reworked taxa in the current study.

The percentage of autochthonous assemblages was calculated by dividing the number of autochthonous specimens by the total number (autochthonous and reworked) of calcareous nannofossils. The complete list of the taxa identified in the Latas section is available in Appendix A.

For the biostratigraphic analysis, bioevents proposed in the Martini (1971) and Agnini et al. (2014) biozonation schemes were used, following the nomenclature of the Lowest Occurrence (LO), Lowest Common Occurrence (LcO), Highest Common Occurrence (HcO), and Highest Occurrence (HO). Also, a few additional stratigraphic biomarkers described by Fornaciari et al. (2010) and Bown and Dunkley Jones (2012) were identified. Additionally, biochronology was developed using the recalibrated ages of Gradstein et al. (2020).

For the paleoenvironmental analysis, only the temperature parameter was considered. The other factors controlling the distribution of calcareous nannofossils could be altered by the variability in the Sabiñánigo Sandstone depositional environment (deltaic environment). Sea surface water temperature indicator taxa were identified and counted in one round, and considering that all genera with similar temperature affinities showed the same trends throughout the section, they were grouped and expressed as a ratio (warm and oligotrophic / temperate and eutrophic taxa). The percentage of *C. floridanus* was calculated by dividing the numbers of this taxon by the total number of autochthonous specimens in each sample.

4 Results

4.1 Calcareous nannofossils assemblages

A total of 60 taxa were identified in the samples from the Latas section (see Appendix A), of which 35 were autochthonous and 25 were reworked. Images of the stratigraphic biomarkers and environmentally significant species are shown in Fig. 2.

In the studied section, the calcareous nannofossil content is predominantly moderate, with some levels of high concentration. The assemblages are characterized by high abundances of *Coccolithus pelagicus*, *Coccolithus formosus*, *Clausicoccus fenestratus*, *Cyclicargolithus floridanus*, and *Zygrhablithus bijugatus*. Other frequently identified species include *Cribrocentrum reticulatum*, *Reticulofenestra bisecta* ($< 10\,\mu m$), and *Reticulofenestra stavensis* ($> 10\,\mu m$).

Reticulofenestra umbilicus ($> 14\,\mu m$) is consistently present throughout the interval, *Braarudosphaera bigelowii* and *Blackites stilus* are common, and *Pemma* sp. and *Helicosphaera bramlettei* are rare and sporadic. Another common genus of the assemblage is *Sphenolithus*, which is mainly represented by *S. radians*, *S. moriformis*, and *S. spiniger*, with a rare occurrence of *S. obtusus*. *Chiasmolithus* is generally low in abundance and is represented by *C. solitus*, *C. medius*, and *C. grandis*.

Reworked taxa occur throughout the Latas section at significant abundances (an average of 54 %). Cretaceous and Paleocene reworked taxa are mainly represented by *Watznaueria barnesiae*, *Cretarhabdus* spp., *Eiffellithus* spp., and *Toweius pertusus* (Fig. 3). A full list of the taxa is given in Appendix A.

Preservation

Calcareous nannofossil preservation is generally moderate to good. This estimation is based on the features observed in taxa susceptible to dissolution and overgrowth, such as *Zygrhablithus bijugatus* and some species of *Reticulofenestra*.

However, some *Chiasmolithus* and *Reticulofenestra umbilicus* specimens were observed with evidence of dissolution in the central area, and only complete specimens with the central cross were considered. Furthermore, in the samples from Interval D, specimens of *Sphenolithus obtusus* show a weak overgrowth at the base.

4.2 Paleoecology

Cribocentrum, *Reticulofenestra*, and *Cyclicargolithus* are cosmopolitan genera related to temperate eutrophic water environments in upwelling and continental discharge zones (Okada and Honjo, 1973; Wei and Wise, 1990; Flores et al., 1995; Toffanin et al., 2011). *Cyclicargolithus floridanus* made up ca. 21 % of the autochthonous assemblage in the Latas section. The genus *Chiasmolithus* is expected to be

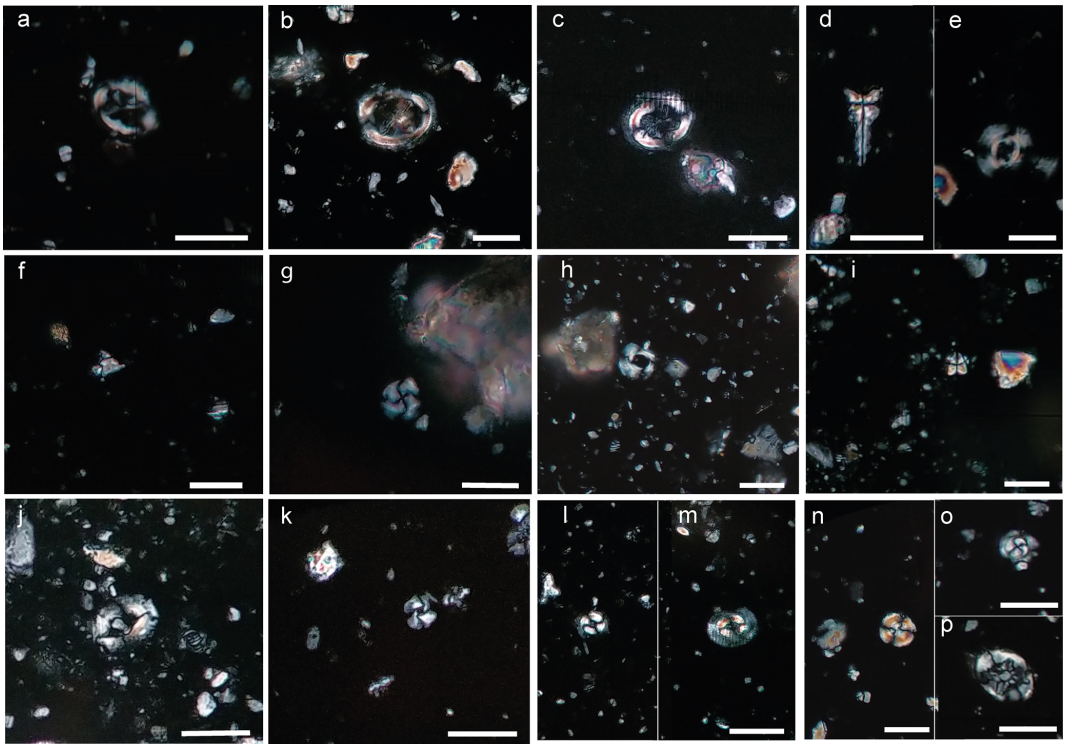

Figure 2. Micrographs of the most significant stratigraphically species in the Latas section: **(a)** *Chiasmolithus solitus* (sample 1); **(b)** *Chiasmolithus grandis* (sample 6); **(c)** *Chiasmolithus medius* (sample 19); **(d)** *Sphenolithus radians*, 0° (sample 12); **(e)** *Reticulofenestra stavensis* (sample 20); **(f)** *Sphenolithus obtusus* (sample 23); **(g)** *Cribrocentrum reticulatum* (sample 23); **(h)** *Reticulofenestra umbilicus* (sample 3); **(i)** *Sphenolithus spiniger*, 0° (sample 2); **(j)** *Helicosphaera bramlettei* (sample 22.2); **(k)** *Cyclicargolithus floridanus* (sample 22); **(l)** *Coccolithus formosus* (sample 23); and **(m)** *Coccolithus pelagicus* (sample 23). Reworked taxa: **(n)** *Watznaueria barnesiae*; **(o)** *Toweius pertusus*; and **(p)** *Eiffellithus* spp. Scale bars are 10 µm.

present for cold, nutrient-rich conditions (Perch-Nielsen, 1985; Intxauspe-Zubiaurre, 2018).

Zygrhablithus bijugatus is a consistent component of the autochthonous assemblage of the Sabiñánigo Sandstone, accounting for ca. 14 % of the total abundance and is usually considered a good indicator of warm and oligotrophic waters (Burky, 1971; Wei and Wise, 1990; Intxauspe-Zubiaurre, 2018; Soták, 2021).

Discoaster represents warm saline oligotrophic conditions (Agnini et al., 2006), and the genus *Blackites* is considered by some authors to be a warm-water indicator (Wei and Wise, 1990; Agnini et al., 2007). Genus *Sphenolithus* develops in warm and oligotrophic waters in open-ocean environments (Wei and Wise, 1990; Aubry, 1992; Intxauspe-Zubiaurre et al., 2017; Soták, 2021).

Coccolithus pelagicus has an important and continuous abundance throughout the study section. At the present day, *C. pelagicus* is found in cold, high-latitude environments (McIntyre and Bé, 1967; Parente et al., 2004; Intxauspe-Zubiaurre, 2018). However, in the Eocene, it appears to have been more abundant at low and mid-latitudes in warm-water conditions (Wei and Wise, 1990). This migration to higher latitudes occurred in the Oligocene, the cause of which is unknown (Haq and Lohmann, 1976; Bukry, 1973). *Coccolithus formosus* is also an indicator of high temperatures; however, it seems more likely to be cosmopolitan (Wei and Wise, 1990).

Therefore, two calcareous nannofossil assemblages with distinct temperature affinities could be identified throughout the formation. The temperate and eutrophic water assemblage, represented by *Cribocentrum* spp., *Reticulofenestra* spp., *Cyclicargolithus floridanus*, and *Chiasmolithus* spp., and the warm and oligotrophic water assemblage, composed of *Zygrhablithus bijugatus*, *Discoaster* spp., *Blackites* spp., *Sphenolithus* spp., *Coccolithus pelagicus*, and *Coccolithus formosus*. The ratio of the abundance between the two groups is plotted in Fig. 3.

4.3 Stratigraphic succession

There appear to be five distinct intervals of the proportion of reworked vs. autochthonous assemblage change across the section studied. Furthermore, these intervals are marked by the presence of significant taxa. These bioevents were recorded according to the nomenclature of the Lowest Occurrence (LO), and Highest Occurrence (HO).

The following paragraphs represent short remarks about the stratigraphic variations in assemblages in the Latas section, which are arranged from base to top.

Interval A (0–2 m) is found at the base of the Latas section. The HO of *Chiasmolithus solitus* occurs within this interval. Other significant taxa such as *Sphenolithus radians* and *S. spiniger* are recorded. The autochthonous fossil assemblages represent an average of 27 %, and reworked taxa made up 73 % of total taxa in this interval.

In interval B (2–13 m), the overall assemblage composition and characteristics are similar to Interval A. The proportion of autochthonous specimens increased to an average of 33 % in Interval B, and reworked taxa slightly decreased to ca. 66 %. In addition, the presence of *Braarudosphaera bigelowii*, *Cribrocentrum reticulatum*, *Chiasmolithus grandis*, and *Sphenolithus moriformis* are recorded, with increasing abundance towards the top of the section.

Within Interval C (13–63 m), the presence of *Chiasmolithus medius*, *Reticulofenestra bisecta*, and *Reticulofenestra stavensis* is recognized. In the same way, the autochthonous taxa increased to 46 %, and reworked specimens represent an average of 54 % of total taxa in this interval.

In Interval D (63–88 m), around 79 and 89 m at the top of the Latas section, the taxon *Sphenolithus obtusus* (LO) is recorded. Furthermore, the LOs of *Helicosphaera bramlettei* and *Pemma basquense* are identified and are consistently present toward the top of the section. The autochthonous fossil assemblage increased slightly to 50 % and reworked taxa constituted an average of 50 % of total taxa. Also, layers of larger benthic foraminifera of the genera *Nummulites* and *Assilina* are recorded between the C and D intervals.

In Interval E (88–130 m), the calcareous nannofossil assemblages are similar to the rest of the section; however, the abundance of taxa decreased slightly towards the top. The autochthonous fossils represent an average of 55 %, and reworked specimens increased to 45 %.

The percentage of reworked and autochthonous assemblage is plotted in Fig. 3. The stratigraphic distribution of the most significant taxa and the bioevents identified are combined to make up a composite chart shown in Fig. 4.

5 Discussion

5.1 Biostratigraphy

For this study, several calcareous nannofossil bioevents have been identified, which in turn correspond to the bioevents and biozonation of Agnini et al. (2014) and Martini (1971). Moreover, some stratigraphic biomarkers described by Fornaciari et al. (2010) and Bown and Dunkey Jones (2012) have been recorded, supporting the correlation with the standard schemes. This study used the same section that was studied for magnetostratigraphy by Oms et al. (2003), and so their magnetostratigraphic results can be combined with our biostratigraphic data.

The HO of *Chiasmolithus solitus* defines the NP16/NP17 boundary (Martini, 1971), and for Agnini et al. (2014), this bioevent corresponds to a range that extends throughout the lower–middle part of zone CNE15 (*D. bisectus–S. obtusus* Concurrent Range Zone (CRZ)). This index species is rare or absent in low-latitude sediments, and other authors have considered this event to be highly diachronous at different latitudes (Perch-Nielsen, 1985; Wei and Wise, 1990; Aubry, 1992; Marino and Flores, 2002; Fornaciari et al., 2010). However, a scarce record of this specimen is identified in the lowest part of the Latas section, above the upper Larrés Marls Formation dated to 40.51 Ma by González-Lanchas et al. (2019). This identification allows us to infer the base of zone CNE15 and the top of zone NP16 in the Bartonian.

The common presence of *Reticulofenestra stavensis* (Levin and Joerger, 1967; Varol, 1989) and *Sphenolithus spiniger* is recorded in the CNE15 zone (*D. bisectus–S. obtusus* CRZ) of Agnini et al. (2014) in the top of chron C18r. This assemblage of *Reticulofenestra stavensis* and *Sphenolithus spiniger* was identified in the middle–lower part of the Latas section. Furthermore, this identification in the Sabiñánigo Sandstone is consistent with chron assignations by Oms et al. (2003), who define the same polarity pattern for this part of the section. *Chiasmolithus grandis* and *Chiasmolithus medius* have also been found in these beds. In addition, a high abundance of *Sphenolithus radians* was observed in the assemblage zone with *C. grandis* and *C. medius*. All these observations support the correspondence of the lowest part of CNE15 and NP17 zones in the Bartonian for this part of the section.

The LO of *Sphenolithus obtusus* developed within NP17 (Bown and Dunkley Jones, 2012) and was dated at 40.13 Ma at the ODP (Ocean Drilling Program) Atlantic site 1052 within a core interval that had an undetermined polarity (Fornaciari et al., 2010) corresponding to the lower part of zone CNE15 (Agnini et al., 2014). The LO of *Sphenolithus obtusus* was observed in the middle–upper part of the Latas section, supporting the change to the base of zone NP17 in the Martini (1971) biozonation scheme and in agreement with the middle–lower part of zone CNE15 in the Bartonian. However, there is only a scarce record of *S. obtusus*, and the specimens are slightly recrystallized. Therefore, this bioevent should be considered with caution. The middle–upper part of the Latas section was assigned to the same chron C18n by Oms et al. (2003).

The HO of *Sphenolithus obtusus* was dated at 38.47 Ma in chron C17r (Agnini et al., 2014) and defines the top of zone CNE15. The LO of *Chiasmolithus oamaruensis* defines the top of zone NP17, according to Martini (1971), and the absence of these taxa in the samples studied allows us to interpret this section as being older than this date (Fig. 4).

Regarding the age of LO of *S. obtusus*, we can obviously say that is younger than 40.073 Ma (age of C18r/C18n2n reversal) and older than 39.666 Ma (C182n/C181r reversal). Precision on the age of this bioevent can be gained by inte-

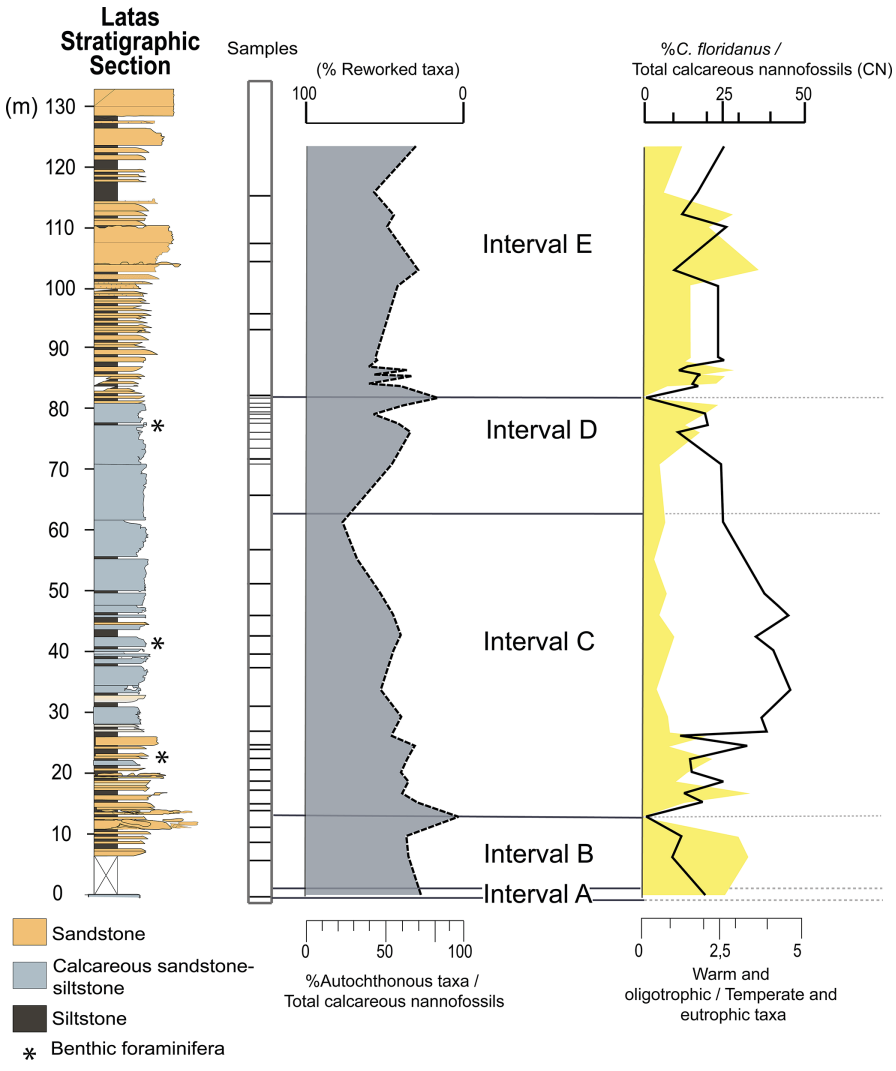

Figure 3. Stratigraphic distribution and relative abundance of the calcareous nannofossils found throughout the studied section. Left: simplified stratigraphy of the Latas section. Center: fluctuations in the abundance of the calcareous nannofossil (CN) assemblage, including the reworked taxa. Intervals of biostratigraphic variation analysis are shown. Right: ratio of temperature indicator taxa and relative abundance of *C. floridanus*. Note that the scale bars are different in each case.

grating (1) its location 10 m above the C18r/C18n reversal in the Latas section and (2) the thickness of the whole C18n2n in Yebra de Basa section, which is 391 m (Vinyoles et al., 2021). Since C18n2n lasts 84 kyr (Gradstein et al., 2020), the age of LO of *S. obtusus* would, at maximum, be a few thousand years younger than C18r/C18n, which would not be differentiated in most oceanic records that are never expanded in this way. In fact, such expanded sections would require further magnetostratigraphic studies to better characterize the magnetization process (delays, reversal timing, etc.). In any case, the Sabiñánigo Sandstone has a large potential for a detailed understanding of Middle Eocene bioevents. In our study, we document that the LO of *S. obtusus* is within C18n2n (ca. 39.866 Ma), which refines the uncertainties in the ODP Atlantic site 1052 (Fornaciari et al., 2010), where this bioevent was correlated with an interval of the core having an undetermined polarity.

5.2 Paleoenvironmental interpretation

Variation in nannofossil abundances and their distribution often reflects changes in the paleoenvironmental conditions of ocean surface waters like changes in temperature, nutrient supply, detrital input, and surface water salinity (Mutterlose et al., 2007). In this study, we focus on the control of seawater temperature on the original structure of nannoplankton, since the other factors controlling the distribution of calcareous nannofossils could be altered by the variability in the Sabiñánigo Sandstone depositional environment (deltaic environment).

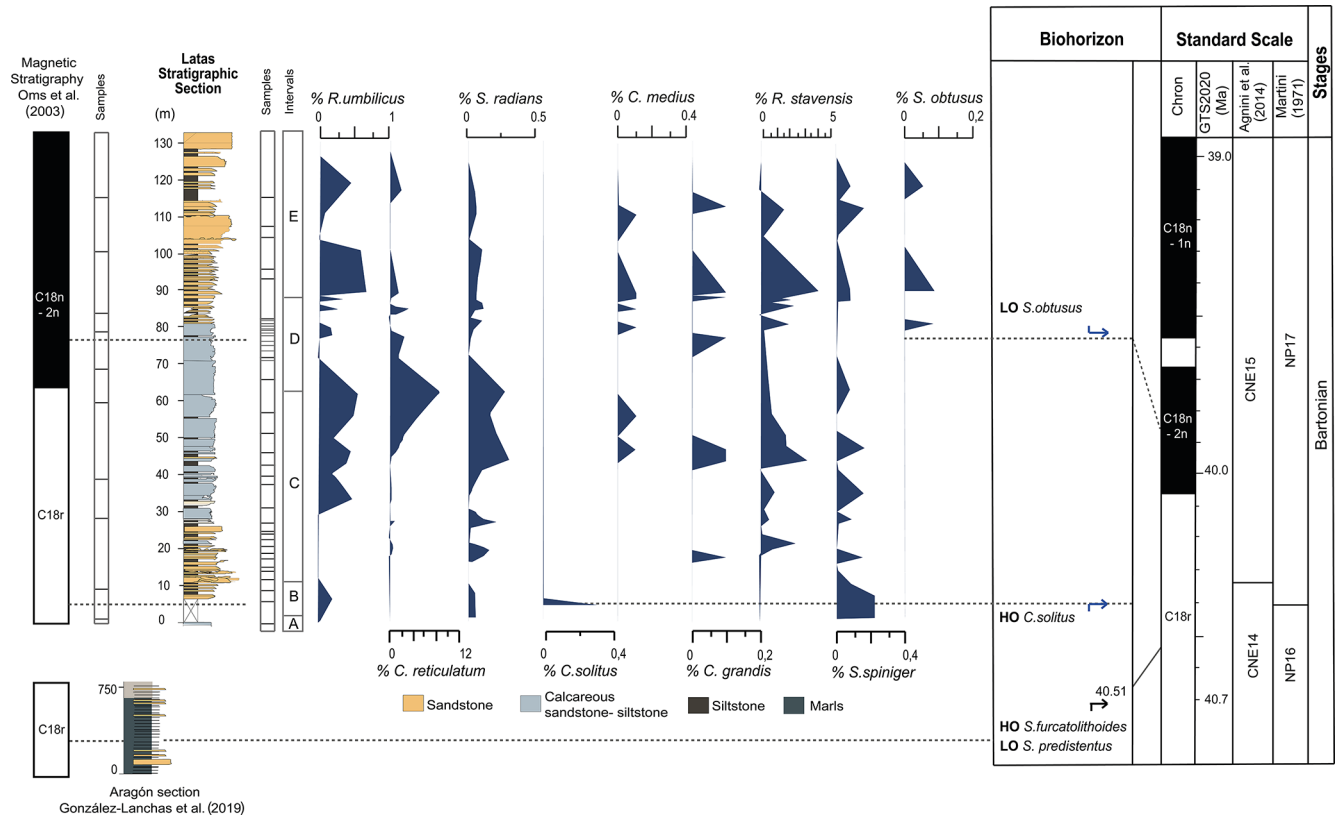

Figure 4. Biostratigraphic events recognized in the Sabiñánigo Sandstone Formation. Left: magnetostratigraphic data of Oms et al. (2003); Aragón stratigraphic section representing the Larrés Marls of González-Lanchas et al. (2019) and the Latas stratigraphic section and nannofossil assemblage variation intervals. Center: calcareous nannofossil abundance and significant taxa in the Latas section. Right: biohorizons and bioevents, where a black arrow indicates a significant bioevent from Agnini et al. (2014) and González-Lanchas et al. (2019), and blue arrows indicate stratigraphic biomarkers from Martini (1971) and Fornaciari et al. (2010). Right: standard biozonation according to Agnini et al. (2014) and correspondence with standard scales of Martini (1971). The magnetostratigraphic assignment for the Middle Eocene is by Gradstein et al. (2020). Eocene stages are shown.

The distribution of calcareous nannofossils along the Latas section clearly shows a pattern conditioned by the sedimentation regime. However, a temperate water and eutrophic assemblage and a warm-water and oligotrophic assemblage are identified.

The comparative record (Fig. 3) shows that the abundance pattern is dominantly from warm and oligotrophic waters throughout the formation, with a slight increase in the abundance of the temperate water nannoflora in the C–D intervals. Despite this, the nannoflora is dominantly from warm and oligotrophic waters showing higher diversity (species abundances) compared to the temperate water assemblage, and the significant levels of benthic foraminifers (*Nummulites* and *Assilina*) also confirm this environmental condition (Hallock, 1985).

The increase in the abundance pattern of surface temperate water assemblage can be explained by the presence of *C. floridanus*. The high record of individuals of *C. floridanus* (r-type opportunistic taxon) may be related to periods of eutrophication (Bown, 1998) rather than a temperature change.

5.3 Calcareous nannofossil assemblages and reworking

One of the significant characteristics of the calcareous nannofossil assemblages found in the Latas section is the high counts of reworked calcareous nannofossils throughout the succession (Fig. 3). The content of allochthonous taxa evidence slightly increases at each interval, moving forwards to the top (Fig. 3). These observations, together with the increase in the abundance of temperate and eutrophic water taxa in the C–D intervals, suggest that seaward-directed currents transported a large volume of reworked material into the ocean, including terrigenous sediments.

This increase in terrigenous sediment can be attributed to an accelerated hydrological cycle that intensified weathering and runoff on land. This scenario of an accelerated hydrological cycle has been documented in several climate events during the Paleocene and Eocene, especially in hyperthermals, which are brief episodes of abrupt global warming (Aubry, 1998; Wing et al., 2005; Held and Soden, 2006; Foreman et al., 2012; Boscolo Galazzo et al., 2013; Carlson and Ca-

ballero, 2017; Intxauspe-Zubiaurre et al., 2017; Honegger et al., 2020).

The Middle Eocene climate optimum (MECO) is considered one of these hyperthermals that lasted ∼ 750 kyr. It ranges from the upper part of chron C18r to subchron C18n.2n at 40–40.75 Ma (Bohaty et al., 2009; Boscolo Galazzo et al., 2014; Giorgini et al., 2019; Henehan et al., 2020; Gradstein et al., 2020). In agreement with our biostratigraphic scheme proposed in this study, the sedimentation of the Sabiñánigo Sandstone Formation took place in this period. This determination agrees with a recent paleoclimate study by Peris-Cabré et al. (2023), which analyzed the effects of the MECO in the Tremp–Jaca Basin and proposed that the Sabiñánigo Sandstone Formation represents the physical evidence of the MECO in the region.

We have no clear evidence of the MECO in the calcareous nannofossil assemblages in the Sabiñánigo Sandstone Formation. However, an effect of this event could have been related to an intensification in the hydrological cycle that resulted in an increased supply of sediments to the ocean. This effect could be recorded in this formation with the high percentage of reworked taxa (around half of the total taxa). Furthermore, the increased terrigenous influx was almost certainly caused by an increase in fluvial freshwater supply into the ocean, which may have altered the salinity and density in shallow seawater and resulted in water column stratification. In addition, the increased continental input could boost nutrient levels leading to eutrophication in shallow seawater (McGonigal and Wise, 2001; Spofforth et al., 2010; Toffanin et al., 2011; Deret et al., 2012; Boscolo Galazzo et al., 2013; Giorgioni et al., 2019). We consider that eutrophication and stratification can be responsible for the increase in the abundance of temperate and eutrophic water taxa found in the C–D intervals, as characterized by the high record of *C. floridanus*.

The abundance of warm and oligotrophic taxa, which should theoretically increase during a hyperthermal event, did not show a clear trend throughout the Latas section but increased slightly at the top of the section. This confirms that the Sabiñánigo Sandstone is influenced by the sedimentation regime and indicates that temperature was not the primary factor controlling the distribution of calcareous nannofossil assemblages in this formation.

6 Conclusions

Two calcareous nannofossil bioevents of the Middle Eocene were identified in the Sabiñánigo Sandstone Formation in the Jaca Basin. The Sabiñánigo Sandstone was deposited during the Middle Eocene, in the Bartonian, from the top of zone NP16 to the base of zone NP17. The HO of *Chiasmolithus solitus* and the LO of *S. obtusus* are found. The age of LO of *S. obtusus* is constrained within the older part of C18n2n (ca. 39.866 Ma), refining the limitations by Fornaciari et al. (2010), where this bioevent was correlated with an interval of the core that had an undetermined polarity.

The paleoenvironmental analysis in the Latas section suggests an environment of warm and oligotrophic waters for the Bartonian period in the Jaca Basin. In addition, this study allowed us to recognize possible eutrophication events characterized by the high record of *C. floridanus*. The eutrophication periods were possibly caused by intensified continental input and freshwater supply to the sea due to the accelerated hydrological cycle.

An effect of the Middle Eocene climate optimum (MECO) could be recorded in the Sabiñánigo Sandstone Formation and expressed by a high proportion of reworked taxa throughout the Latas section. This could result from intensification of the hydrological cycle on land, intensified weathering, runoff, and increased continental sediment and freshwater supply to the sea.

Appendix A: Taxonomic references

The following lists include all taxa (autochthonous and reworked) present in the Latas section and cited in the paper. The references used for the identification of the taxa are indicated in Sect. 3, and the Nannotax website also includes a bibliography giving all the taxonomic references cited in this list.

A1 Identified taxa

Blackites Hay and Towe 1962

Blackites inversus (Bukry and Bramlette, 1969) Bown and Newsam 2017

Blackites stilus Bown 2005

Blackites subtilis Bown and Newsam 2017

Blackites tenuis (Bramlette and Sullivan, 1961) Sherwood 1974

Braarudosphaera Deflandre 1947

Braarudosphaera bigelowii (Gran and Braarud 1935) Deflandre 1947

Braarudosphaera sequela Self-Trail 2011

Chiasmolithus Hay et al. 1966

Chiasmolithus medius Perch-Nielsen, 1971

Chiasmolithus grandis (Bramlette and Riedel 1954) Radomski 1968

Chiasmolithus modestus Perch-Nielsen, 1971

Chiasmolithus solitus (Bramlette and Sullivan 1961) Locker 1968

Clausicoccus Prins, 1979

Clausicoccus fenestratus (Deflandre and Fert 1954) Prins 1979

Coccolithus Schwartz 1894

Coccolithus formosus (Kamptner 1963) Wise 1973

Coccolithus pelagicus (Wallich 1877) Schiller 1930

Cribrocentrum Perch-Nielsen, 1971

Cribrocentrum reticulatum (Gartner and Smith 1967) Perch-Nielsen 1971

Cyclicargolithus Bukry 1971

Cyclicargolithus floridanus (Roth and Hay, in Hay et al. 1967) Bukry 197

Discoaster Tan 1927

Discoaster barbadiensis Tan 1927

Discoaster gemmifer Stradner 1961

Discoaster binodosus Martini 1958

Discoaster tanii Bramlette and Riedel 1954

Discoaster williamsii Bown and Dunkley Jones 2012

Helicosphaera Kamptner 1954

Helicosphaera bramlettei (Müller 1970) Jafar and Martini 1975

Micrantholithus (Deflandre in Deflandre and Fert 1954)

Micrantholithus astrum Bown 2005

Pemma Klumpp 1953

Pemma basquense (Martini 1959) Báldi-Beke 1971

Reticulofenestra Hay et al. 1966

Reticulofenestra dictyoda (Deflandre in Deflandre and Fert, 1954) Stradner in Stradner and Edwards, 1968

Reticulofenestra bisecta (Hay, Mohler and Wade, 1966) Roth, 1970

Reticulofenestra stavensis (Levin and Joerger, 1967) Varol, 1989

Reticulofenestra umbilicus (Levin 1965) Martini and Ritzkowski 1968

Sphenolithus Deflandre in Grasse 1952

Sphenolithus moriformis (Bronnimann and Stradner 1960) Bramlette and Wilcoxon, 1967

Sphenolithus radians Deflandre in Grasse 1952

Sphenolithus spiniger Bukry 1971

Sphenolithus obtusus Bukry 1971

Zygrhablithus Deflandre 1959

Zygrhablithus bijugatus (Deflandre in Deflandre and Fert 1954) Deflandre, 1959

A2 Cenozoic reworked taxa

Chiasmolithus Hay et al. 1966

Chiasmolithus bidens (Bramlette and Sullivan 1961) Hay and Mohler 1967

Discoaster Tan 1927

Discoaster araneus Bukry 1971

Discoaster backmanii Agnini et al. 2008

Discoaster lodoensis Bramlette and Riedel 1954

Discoaster multiradiatus Bramlette and Riedel 1954

Prinsius Hay and Mohler 1967

Prinsius martinii (Perch-Nielsen 1969) Haq 1971

Toweius Hay and Mohler 1967

Toweius gammation Romein 1979

Toweius pertusus (Sullivan 1965) Romein 1979

Tribrachiatus Shamrai 1963

Tribrachiatus orthostylus Shamrai 1963

A3 Mesozoic reworked taxa

Arkhangelskiella Bekshina 1959

Arkhangelskiella cymbiformis Vekshina 1959

Broinsonia Bukry 1969

Cretarhabdus Bramlette and Martini 1964

Cruciplacolithus Hay and Mohler in Hay et al. 1967

Cruciplacolithus edwardsii Romein 1979

Eiffellithus Reinhardt 1965

Eprolithus Stover 1966

Eprolithus rarus Varol 1992

Microrhabdulus Deflandre 1959

Microrhabdulus undosus Perch-Nielsen 1973

Manivitella Thierstein 1971

Manivitella pemmatoidea (Deflandre in Manivit 1965) Thierstein, 1971

Micula Vekshina 1959

Placozygus Hoffman 1970

Placozygus spiralis (Bramlette and Martini 1964) Hoffmann 1970

Russellia Risatti 1973

Russellia laswellii Risatti 1973

Tetrapodorhabdus Black 1971

Tetrapodorhabdus decorus (Deflandre in Deflandre and Fert 1954) Wind and Wise 1983

Watznaueria Reinhardt 1964

Watznaueria barnesiae (Black in Black and Barnes 1959) Perch-Nielsen 1968

Zeugrhabdotus Reinhardt 1965

Zeugrhabdotus embergeri (Noël 1959) Perch-Nielsen 1984

Data availability. Biostratigraphic data generated in this study are available in Supplement. All the slides containing nannofossils studied in this contribution are stored in the micropaleontological collection of the University of Salamanca, Spain.

Supplement. The supplement related to this article is available online at: https://doi.org/10.5194/jm-43-55-2024-supplement.

Author contributions. OO conceived the project and contributed to the interpretation. ERL, ER, and HBR performed the fieldwork and sampling. ERL performed the sample preparation and light microscope imaging. The species were determined by ERL under the supervision of JAF. AGL contributed to the review of biostratigraphic data and edited the article. ERL prepared the paper and figures, with contributions from JAF and OO. All authors contributed to the interpretation of the data.

Competing interests. The contact author has declared that none of the authors has any competing interests.

Disclaimer. Publisher's note: Copernicus Publications remains neutral with regard to jurisdictional claims made in the text, published maps, institutional affiliations, or any other geographical representation in this paper. While Copernicus Publications makes every effort to include appropriate place names, the final responsibility lies with the authors.

Acknowledgements. We would like to thank the Master of Earth Sciences: Environmental and Applied Geology of the University of Salamanca for supporting this article. The authors would like to thank Jeremy Young and one anonymous referee for dedicating their time to reviewing the paper and for their valuable suggestions that helped improve this work.

Financial support. This research has been supported by the Ministerio de Ciencia e Innovación (grant no. PGC2018-101575-B-I00).

Review statement. This paper was edited by Emanuela Mattioli and reviewed by Jeremy Young and one anonymous referee.

References

Agnini, C., Muttoni, G., Kent, D. V., and Rio, D.: Eocene biostratigraphy and magnetic stratigraphy from Possagno, Italy: The calcareous nannofossil response to climate variability, Earth Planet. Sc. Lett., 241, 815–830, https://doi.org/10.1016/j.epsl.2005.11.005, 2006.

Agnini, C., Fornaciari, E., Rio, D., Tateo, F., Backman, J., and Giusberti, L.: Responses of calcareous nannofossil assemblages, mineralogy, and geochemistry to the environmental perturbations across the Paleocene/Eocene boundary in the Venetian Pre-Alps, Mar. Micropaleontol., 63, 19–38, https://doi.org/10.1016/j.marmicro.2006.10.002, 2007.

Agnini, C., Fornaciari, E., Raffi, I., Catanzariti, R., Pälike, H., Backman, J., and Rio, D.: Biozonation and biochronology of Paleogene calcareous nannofossils from low and middle latitudes, Newsl. Stratigr., 47, 131–181, https://doi.org/10.1127/0078-0421/2014/0042, 2014.

Aubry, M. P.: Late Paleogene calcareous nannoplankton evolution: a tale of climatic deterioration, in: Eocene–Oligocene climatic and biotic evolution, edited by: Prothero, D. R. and Berggren, W. A., Eocene–Oligocene Climatic and Biotic Evolution, Princeton, Princeton University Press, 135, 272–309, https://doi.org/10.1515/9781400862924, 1992.

Aubry, M. P.: Early Paleogene Calcareous nannoplankton evolution: a tale of climatic amelioration, in: Late Paleocene–early Eocene Biotic and Climatic Events in the Marine and Terrestrial Records, edited by: Aubry, M.-P., Lucas, S., and Berggren, W. A., Columbia University Press, 158–201, ISBN 9780231102384, 1998.

Bauer, F. U.: The Sabiñánigo Sandstone Succession, Jaca basin, Southern Pyrenees, NE-Spain, A Depositional model, PhD thesis, University of Heidelberg, 184 pp., https://doi.org/10.11588/heidok.00007977, 2007.

Bohaty, S., Zachos, J. C., Florindo, F., and Delaney, M. L.: Coupled greenhouse warming and deep-sea acidification in the Middle Eocene, Paleoceanogr. Paleocl., 24, PA2207, https://doi.org/10.1029/2008PA001676, 2009.

Boscolo Galazzo, F., Giusberti, V., Luciani, E., and Thomas, E.: Paleoenvironmental changes during the Middle Eocene Climatic Optimum (MECO) and its aftermath: The benthic foraminiferal record from the Alano sec-

tion (NE Italy), Palaeogeogr. Palaeoecl., 378, 22–35, https://doi.org/10.1016/j.palaeo.2013.03.018, 2013.

Boscolo Galazzo, F., Thomas, E., Pagani, M., Warren, C., Luciani, V., and Giusberti, L.: The middle Eocene climatic optimum (MECO): A multiproxy record of paleoceanographic changes in the southeast Atlantic (ODP Site 1263, Walvis Ridge), Palaeogeogr. Palaeoecl., 29, 1143–1161, https://doi.org/10.1002/2014PA002670, 2014.

Bown, P. R.: Calcareous Nannofossil Biostratigraphy, British micropaleontological society publication series, Chapman, and Hall, Kluwer Academic and Lipincott-Raven Publishers, London, Springer, 16–28, ISBN 109401060568, 1998.

Bown, P. R. and Dunkley Jones, T.: Calcareous nannofossils from the Paleogene equatorial Pacific (IODP Expedition 320 Sites U1331-1334), J. Nannoplank. Res., 32, 3–51, ISSN 1210-8049, 2012.

Boya, S.: El sistema deltaico de la Arenisca de Sabiñánigo y la continentalización de la cuenca de Jaca, Tesis de la Universitat Autònoma de Barcelona, 207 pp., http://hdl.handle.net/10803/665452 (last access: 15 January 2024), 2018.

Bukry, D.: Cenozoic calcareous nannofossils from the Pacific Ocean, Transactions of San Diego Society of Natural History, 16, 303–327, https://doi.org/10.5962/bhl.part.15464, 1971.

Bukry, D.: Low latitude coccolith biostratigraphic zonation, in: Proceedings of the Deep-Sea Drilling Project, edited by: Edgar, N. T. and Saunders, J. B., Initial Reports, 15, Washington, DC, US Government Printing Office, 685–703, 1973.

Canudo, J. I. and Molina, E.: Biocronología con foraminíferos planctónicos de la secuencia deposicional de Jaca (Pirineo aragonés): Eoceno medio y superior, Congreso Geológico de España, Comunicaciones, 1, 273–276, 1988.

Cámara, P. and Klimowitz, J.: Interpretación geodinámica de la vertiente centro-occidental surpirenaica (cuencas de Jaca-Tremp), Estud. Geol.-Madrid, 41, 391–404, https://doi.org/10.3989/egeol.85415-6720, 1985.

Cámara, P. and Flinch J. F.: The Southern Pyrenees: a salt-based fold and thrust belt, in: Permo-Triassic Salt Provinces of Europe, North Africa and the Atlantic Margins, edited by: En Soto, J. I., Flinch, J. F., and Tari, G., Tectonics and Hidrocarbon potencial, Cap, 18, 395–413, https://doi.org/10.1016/B978-0-12-809417-4.00019-7, 2017.

Carlson, H. and Caballero, R.: Atmospheric circulation and hydroclimate impacts of alternative warming scenarios for the Eocene, Clim. Past, 13, 1037–1048, https://doi.org/10.5194/cp-13-1037-2017, 2017.

Dedert, M., Stoll, H. M., Kroon, D., Shimizu, N., Kanamaru, K., and Ziveri, P.: Productivity response of calcareous nannoplankton to Eocene Thermal Maximum 2 (ETM2), Clim. Past, 8, 977–993, https://doi.org/10.5194/cp-8-977-2012, 2012.

Flores, J. A. and Sierro, F. J.: Revised technique for calculation of calcareous nannofossil accumulation rates, Micropaleontology, 43, 321–324, https://doi.org/10.2307/1485832, 1997.

Flores, J. A., Sierro, F. J., and Raffi, I.: Evolution of the calcareous nannofossil assemblage as a response to the paleoceanographic changes in the eastern equatorial Pacific Ocean from 4 to 2 Ma, Leg 138, sites 849 and 852, in: Proceedings of the Ocean Drilling Program, edited by: Pisias, N. G., Mayer, L. A., Janecek, T. R., Palmer-Julson, A., and van Andel, T. H., Scientific Results 138, College Station, Texas, 163–176, 1995.

Foreman, B. Z., Heller, P. L., and Clementz, M. T.: Fluvial response to abrupt global warming at the Palaeocene/Eocene boundary, Nature, 491, 92–95, https://doi.org/10.1038/nature11513, 2012.

Fornaciari, E., Agnini, C., Catanzariti, R., Rio, D., Bolla, E. M., and Valvasoni, E.: Mid-latitude calcareous nannofossil biostratigraphy and biochronology across the middle to late Eocene transition, Stratigraphy, 7, 229–264, 2010.

Gil-Peña, I., Montes-Santiago M. J., and Malagón, J.: Mapa geológico de la Hoja no 177, 29-09 (Sabiñánigo), Mapa Geológico de España E, 1 : 50 000, Segunda Serie (MAGNA), Primera edición, IGME, 1990.

Giorgioni, M., Jovane, L., Rego, E. S., Rodelli, D., Frontalini, F., Coccioni, R., Catanzariti, R., and Özcan, E.: Carbon cycle instability and orbital forcing during the Middle Eocene Climatic Optimum, Sci. Rep., 9, 9357, https://doi.org/10.1038/s41598-019-45763-2, 2019.

González-Lanchas, A., Remacha, E., Oms, O., Sierro, F. J., and Flores, J. A.: Middle Eocene calcareous nannofossils in the Jaca transect (South-central Pyrenees Eocene Basin, Aragón River valley, Huesca), Span. J. Palaeontol., 34, 229–240, https://doi 10.7203/sjp.34.2.16096, 2019.

Gradstein, F., Ogg, J. G., Schmitz, M. D., and Ogg, G. M., Geologic Time Scale, Elsevier, 2, ISBN 978-0-12-824360-2, 2020.

Hallock, P.: Why are larger foraminifera large?, Paleobiology, 11, 195–208, https://www.jstor.org/stable/2400527 (last access: 1 April 2024), 1985.

Haq, B. U. and Lohman, G. P.: Early Cenozoic calcareous nannoplankton biogeography of the Atlantic Ocean, Mar Micropaleontol., 1, 119–194, https://doi.org/10.1016/0377-8398(76)90008-6, 1976.

Hehuwat, F.: The Transition from marine to continental sedimentation in the Eoceno of Guarda synclinorium, Huesca province, Spain, Thesis Utrecht, 1970.

Held, I. M. and Soden, B. J.: Robust responses of the hydrological cycle to global warming, J. Climate, 19, 5686–5699, https://doi.org/10.1175/JCLI3990.1, 2006.

Henehan, M. J., Edgar, K. M., Foster, G. L., Penman, D. E., Hull, P. M., Greenop, R., and Pearson, P. N.: Revisiting the Middle Eocene Climatic Optimum "Carbon Cycle Conundrum" with new estimates of atmospheric pCO2 from boron isotopes, Paleoceanogr. Paleocl., 35, e2019PA003713, https://doi.org/10.1029/2019PA003713, 2020.

Hogan P. J. and Burbank D.: Evolution of the Jaca piggyback basin and emergence of the External Sierra, southern Pyrenees, in: Tertiary Basins of Spain: the Stratigraphic Record of Crustal Kinematics, edited by: Friend, P. F. and Dabrio, J. C., Cambridge University Press, Cambridge, 153–160, https://doi.org/10.1017/CBO9780511524851.023, 1996.

Honegger, L., Adatte, T., Spangenberg, J. E., Rugenstein, J. K. C., Poyatos-Moré, M., Puigdefàbregas, C., Chanvry, E., Clark, J., Fildani, A., Verrechia, E., Kouzmanov, K., Harlaux, M., and Castelltort, S.: Alluvial record of an early Eocene hyperthermal within the Castissent Formation, the Pyrenees, Spain, Clim. Past, 16, 227–243, https://doi.org/10.5194/cp-16-227-2020, 2020.

Intxauspe-Zubiaurre, B.: Análisis de la Dinámica Oceánica Superficial en la Cuenca Vascocantábrica durante Tres Eventos Hipertermales del Eoceno a través de nanofósiles calcáreos, Tesis doctora l, UPV/EHU, 238 pp., http://hdl.handle.net/10810/32107 (last access: 15 January 2024), 2018.

Intxauspe-Zubiaurre, B., Flores, J., and Payros, A.: Variations to calcareous nannofossil $CaCO_3$ content during the middle Eocene C21r-H6 hyperthermal event ($\sim$ 47.4 Ma) in the Gorrondatxe section (Bay of Biscay, Western Pyrenees), Palaeogeogr. Palaeocl., 487, 296–306, https://doi.org/10.1016/j.palaeo.2017.09.015, 2017.

Labaume, P. and Teixell, A.: 3D structure of subsurface thrusts in the eastern Jaca Basin, southern Pyrenees, Geolog. Ac., 16, 477–498, https://doi.org/10.1344/GeologicaActa2018.16.4.9, 2018.

Labaume, P., Séguret, M., and Seyve, C.: Evolution of a turbiditic foreland basin and analogy with an accretionary prism: Example of the Eocene South-Pyrenean basin, Tectonics, 4, 661–685, https://doi.org/10.1029/TC004i007p00661, 1985.

Lafont, F.: Influences relatives de la subsidence et de l'eustatisme sur la localisation et la géométrie des réservoirs d'un systéme deltaïque, Example de l'Eocene du Bassin de Jaca (Pyrenees Espagnoles), PhD thesis, Université de Rennes I, 288 pp., https://theses.hal.science/tel-00653783 (last access: 1 April 2024), 1994.

Marino, M. and Flores, J. A.: Middle Eocene to Early Oligocene calcareous nannofossil stratigraphy at Leg 177 Site 1090, Mar. Micropaleontol., 45, 383–398, https://doi.org/10.1016/S0377-8398(02)00036-1, 2002.

Martini, E.: Standard Tertiary and Quaternary calcareous nannoplankton zonation, in: Proceedings 2nd International Conference Planktonic Microfossils Roma, edited by: Farinacci, A., Tecnoscienza, Rome, 2, 739–785, 1971.

McIntyre, A. and Bé, A.: Modern Coccolithophores of the Atlantic Ocean. I. Placolith and Cyrtholiths, Deep-Sea Res., 14, 561–597, https://doi.org/10.1016/0011-7471(67)90065-4, 1967.

McGonigal, K. L. and Wise Jr., S. W.: Eocene calcareous nannofossil biostratigraphy and sediment accumulation of turbidite sequences on the Iberia Abyssal Plain, ODP Sites 1067–1069, in: Proceedings ODP, edited by: Beslier, M. O., Whitmarsh, R. B., Wallace, P. J., and Girardeau, J., Scientific Results, 173, 1–35, 2001.

Moebius, I., Friedrich, O., and Scher, H.: Changes in Southern Ocean bottom water environments associated with the Middle Eocene Climatic Optimum (MECO), Palaeogeogr. Palaeocl., 405, 16–27, https://doi.org/10.1016/j.palaeo.2014.04, 2014.

Montes, M. J.: Estratigrafia del Eoceno-Oligoceno de la Cuenca de Jaca (Sinclinorio del Guarga), Tesis Universitat de Barcelona, 365 pp., https://dialnet.unirioja.es/servlet/tesis?codigo=235289 (last access: 1 April 2024), 2002.

Mutterlose, J., Linnert, C., and Norris, R.: Calcareous nannofossils from the Paleocene-Eocene Thermal Maximum of the equatorial Atlantic (ODP Site 1260B): Evidence for tropical warming, Mar. Micropaleontol., 65, 13–31, https://doi.org/10.1016/j.marmicro.2007.05.004, 2007.

Okada, H. and Honjo, S.: Distribution of coccolithophorids in marginal seas along the western Pacific Ocean and in the Red Sea, Mar. Biol., 31, 271–285, https://doi.org/10.1007/BF00387154, 1975.

Oms, O., Dinarès-Turell, J., and Remacha, E.: Magnetic stratigraphy from deep clastic turbidites: an example from the Eocene Hecho Group (southern Pyrenees), Stud. Geophys. Geod., 47, 275–288, https://doi.org/10.1023/A:1023719607521, 2003.

Parente, A., Cachao, M., Baumann, K.-H., de Abreu, L., and Ferreira, J.: Morphometry of Coccolithus pelagicus s.l. (Coccolithophore, Haptophyta) from offshore Portugal during the last 200 kyr, Micropaleontology, 50, 107–120, https://www.jstor.org/stable/4097106 (last access: 1 April 2024), 2004.

Perch-Nielsen, K.: Cenozoic calcareous nannofossils, edited by: Saunders, J. B. and Perch-Nielsen, K., Plankton stratigraphy, Cambridge University Press, UK, 427–554, 1985.

Peris Cabré, S., Valero, L., Spangenberg, J. E., Vinyoles, A., Verité, J., Adatte, T., Tremblin, M., Watkins, S., Sharma, N., Garcés, M., Puigdefàbregas, C., and Castelltort, S.: Fluvio-deltaic record of increased sediment transport during the Middle Eocene Climatic Optimum (MECO), Southern Pyrenees, Spain, Clim. Past, 19, 533–554, https://doi.org/10.5194/cp-19-533-2023, 2023.

Puigdefábregas, C.: La sedimentación molásica en la cuenca de Jaca. Monografías del Instituto de Estudiós Pirenaicos, num. 104, CESIC, Jaca, http://hdl.handle.net/10261/82989 (last access: 1 April 2024), 1975.

Remacha, E. and Picart, J.: El complejo turbidítico de Jaca y el delta de la arenisca de Sabiñánigo, Excursion Guidebook 8, 1er. Congresso del Grupo Español del Terciario, Vic Universitat de Barcelona, https://books.google.es/books/about/El_complejo_turbiditico_de_Jaca_y_el_del.html?id=uJpG0AEACAAJ&redir_esc=y (last access date: 1 April 2024), 1991.

Remacha, E., Arbués, P., and Carreras, M.: Precisiones sobre los límites de la secuencia deposicional de Jaca. Evolucioń de las facies desde la base de la secuencia hasta el techo de la Arenisca de Sabiñánigo, Boletín Geológico y Minero, 98, 40–48, ISSN 0366-0176, 1987.

Remacha, E., Oms, O., and Coello, J.: The Rapitán turbidite channel and its related eastern levee-over bank deposits, in: Eocene Hecho group, South-central Pyrenees, Spain, edited by: Pickering, K. T., Hiscott, R. N., Kenyon, N. H., Ricci Lucchi, F., and Smith, R. D. A., Atlas of Deep Water Environments, Springer, Dordrecht, https://doi.org/10.1007/978-94-011-1234-5_22, 1995.

Remacha, E., Gual, G., Bolaño, F., Arcuri, M., Oms, O., Climent, F., Crumeyrolle, P., Fernandez, L. P., Vicente, J. C., and Suarez, J.: Sand-rich turbidite systems of the Hecho Group from slope to the basin plain, Facies, stacking patterns, controlling factors, and diagnostic features, Barcelona, American Association of Petroleum Geologists (AAPG), International Conference and Exhibition, Field Trip 12 Guidebook, 2003.

Roigé, M.: Procedéncia i evolució dels sistemes sedimentaris de la conca de Jaca (conca d'avantpaís Sudpirinenca): Interacció entre diverses árees font en un context tectónic actiu: PhD Thesis, Universitat Autónoma de Barcelona, 314 pp., http://hdl.handle.net/10803/565902 (last access: 1 April 2024), 2018.

Seguret, M.: Etude tectonique des nappes et séries décollées de la partie centrale du versant sud des Pyrénées, Publ. Ustela, série Géol, Struct. No 2, Montpellier, 155 pp., https://www.sudoc.fr/012768294 (last access: 1 April 2024), 1972.

Soler-Sampere, M. and Puigdefábregas, C.: Líneas generales de la Geología del Alto Aragón Occidental, Pirineos, 96, 5–20, http://hdl.handle.net/10261/93785 (last access: 1 April 2024), 1970.

Stokke, E., Jones, M., Tierney, J., Svensen, H., and Whiteside, J.: Temperature changes across the Paleocene-Eocene Thermal Maximum – a new high-resolution TEX86 temperature record from the Eastern North Sea Basin, Earth Planet. Sc. Lett., 544, 116388, https://doi.org/10.1016/j.epsl.2020.116388, 2020.

Soták, J., Elbra, T., Pruner, P., Antolíková, S., Schnabl, P., Biroň, A., Kdýr, Š., and Milovský, R.: End-Cretaceous to middle Eocene events from the Alpine Tethys: Multi-proxy data from a reference section at Kršteňany (Western Carpathians), Palaeogeogr. Palaeocl., 579, 110571, https://doi.org/10.1016/j.palaeo.2021.110571, 2021.

Spofforth, D. J. A., Agnini, C., Pälike, H., Rio, D., Fornaciari, E., Giusberti, L., and Muttoni, G.: Organic carbon burial following the middle Eocene climatic optimum in the central western Tethys, Paleoceanogr. Paleocl., 25, 11, https://doi.org/10.1029/2009PA001738, 2010.

Teixell, A.: The Ansó transect of the southern Pyrenees: basement and cover thrust geometries, J. Geol. Soc. London, 153, 301–310, https://doi.org/10.1144/gsjgs.153.2.030, 1996.

Teixell, A. and García- Sansegundo, J.: Estructura del sector central de la Cuenca de Jaca (Pirineos meridionales), Revista de la Sociedad Geológica Española, 8, 215–228, 1995.

Toffanin, F., Agnini, C., Fornaciari, E., Rio, D., Giusberti, L., Luciani, V., Spofforth, D. J. A., and Pälike, H.: Changes in calcareous nannofossil assemblages during the Middle Eocene Climatic Optimum: Clues from the central-western Tethys (Alano section, NE Italy), Mar. Micropaleontol., 81, 22–31, https://doi.org/10.1016/j.marmicro.2011.07.002, 2011.

Vinyoles, A., López-Blanco, M., Garcés, M., Arbués, P., Valero, L., Beamud, E., and Cabello, P.: 10 Myr evolution of sedimentation rates in a deep marine to non-marine foreland basin system: Tectonic and sedimentary controls (Eocene, Tremp–Jaca Basin, Southern Pyrenees, NE Spain), Basin Res., 33, 447–477, https://doi.org/10.1111/bre.12481, 2021.

Wei, W. and Wise, S. W.: Biogeographic gradients of middle Eocene-Oligocene calcareous nannoplankton in the South Atlantic Ocean, Palaeogeogr. Palaeocl., 79, 29–61, https://doi.org/10.1016/0031-0182(90)90104-F, 1990.

Wing, S. L., Harrington, G. J., Smith, F. A., Bloch, J. I., Boyer, D. M., and Freeman, K. H.: Transient floral change and rapid global warming at the Paleocene-Eocene Boundary, Science, 310, 993–996, https://doi.org/10.1126/science.1116913, 2005.

Zachos, J. C., Dickens, G. R., and Zeebe, R. E.: An early Cenozoic perspective on greenhouse warming and carbon-cycle dynamics, Nature, 451, 279–293, https://doi.org/10.1038/nature06588, 2008.